CO_2 Conversion via DBD Coupled with Iron Foam

Qi Li, Na Liu*, Sai Li*, Yuhang Wang, Guangning Liao, Zeyi Xin

School of Chemistry and Chemical Engineering, Xi'an University of Science and Technology, Xi'an, 710054, China

* Corresponding author: liuna307@126.com (N. Liu), saili@xust.edu.cn (S. Li).

Keywords: Non-thermal plasma; DBD; CO_2 conversion; Iron foam; Stability

Abstract: Dielectric barrier discharge plasma (DBD) may directly convert CO_2 into CO and O_2 using a catalyst at ambient temperature and pressure. This study investigated the effect of iron foam filled into a DBD reactor on CO_2 conversion efficiency. As input power rises, the CO_2 conversion rate escalates. In comparison to the empty reactor, iron foam markedly enhances CO_2 conversion performance, achieving a CO_2 conversion rate of up to 30% and an energy efficiency of up to 2.0%. The thermal stability of the iron foam was evaluated at 80 W power, revealing that it could sustain high catalytic activity for an extended duration. Furthermore, residence time also significantly influences CO_2 conversion. The CO_2 conversion rate progressively rises with extended residence time, whilst energy efficiency diminishes. Nevertheless, during brief residence time, energy efficiency may attain as much as 3.5%.

1. Introduction

The ongoing utilization of fossil energy sources renders CO_2 emissions a significant global issue.[1] CO_2, the preeminent greenhouse gas, is released in substantial amounts, contributing to global warming. It has also resulted in several environmental issues, including glacial melting, elevated sea levels, droughts, and severe weather phenomena such as floods.[2]

To address the environmental issues resulting from CO_2 emissions, transforming CO_2 into valuable compounds has emerged as a significant task. Nonetheless, CO_2 has significant thermodynamic stability[3], and its breakdown necessitates temperatures above 2000°C[4]. This decomposition process results in elevated energy consumption and diminished efficiency[5], making it challenging to attain effective CO_2 conversion.

In contrast,, non-thermal plasma technology (NTP) has garnered significant interest as an alternative approach for CO_2 conversion, owing to its capability to directly transform CO_2 into CO and other highly valuable compounds[5]. The distinguishing feature of NTP is its capacity to produce energetic electrons that can promote various chemical processes at ambient temperature and pressure[6]. Furthermore, the electron energy and electron temperatures in NTP are exceedingly elevated, with usual electron energies fluctuating from 1 - 10 eV[7]. Presently, non-thermal plasma methodologies applicable for laboratory investigations encompass glow discharges, sliding arc discharges, microwave discharges, radiofrequency discharges, and dielectric barrier discharges[8, 9]. Among them, dielectric barrier discharge (DBD) is particularly advantageous for CO_2 conversion owing to its stable and uniform discharge, ease of adjustment of reaction conditions, and cost-effectiveness.[10-13]

Current research indicates that CO_2 conversion in individual DBD reactors has been documented. Nevertheless, the conversion rates of CO_2 are often minimal. Consequently, a combination of DBD and catalyst was employed to create a synergistic effect with the purpose of enhancing the CO_2 conversion rate. Ray et al.[14] examined the influence of metal oxides supported by γ-Al_2O_3 catalysts on CO_2 conversion efficiency, demonstrating that the CO_2 conversions achieved with both NiO/Al_2O_3 and CuO/Al_2O_3 were markedly superior to those obtained in the absence of the catalyst. Mei et al.[15] integrated plasma with photocatalysts and discovered that the conversion of CO_2 and energy efficiency could be markedly enhanced by their synergistic interaction. Zhu et al.[7] examined the

  DOI: 10.25236/icmmct.2025.001

influence of filler materials on CO_2 conversion utilizing a DBD reactor containing copper and nickel foam. The findings indicated that the incorporation of foam metal might significantly enhance CO_2 conversion. These investigations have validated that the synergistic interaction between the catalyst and DBD can significantly enhance CO_2 conversion efficiency.

Nevertheless, the majority of the aforementioned studies concentrate on CO_2 conversion, with limited subsequent study on the stability and catalytic efficacy of catalysts. This study examined the synergistic effect of foamed iron and DBD on CO_2 conversion performance at ambient temperature and pressure, and investigated the impact of the thermal stability and residence time of foamed iron on CO_2 conversion. The alterations of foamed iron before and after the CO_2 conversion reaction were examined using XRD, XPS, and SEM techniques. The reaction mechanism of CO_2 co-conversion using iron foam and plasma was examined in conjunction with the experimental data.

2. Experimental

2.1 Catalyst Pretreatment

Iron foam was acquired from Kunshan Shangte New Material Co. Ltd, with a metal content of around 99.9 wt%, a thickness of 1 mm, and a porosity of 110 PPI. Pre-treat the iron foam prior to utilization. Initially, the iron foam was trimmed to the requisite dimensions and immersed in 100 ml of deionised water for ultrasonication for a duration of 10 minutes. The material was thereafter put into 100 ml of anhydrous ethanol for ultrasonication for 10 minutes, followed by drying in an oven at 80°C for components. The reactor packed with iron foam is subsequently designated as IF-DBD.

2.2 Experimental Setup

The DBD reactor employed in the studies is a coaxial cylindrical configuration, primarily composed of dielectric material, an inner electrode, and an outside electrode. The dielectric material is a hollow cylindrical quartz tube, with an inner diameter of 15 mm, an outer diameter of 18 mm, and a length of 300 mm. The quartz tube features an input and an outlet on either side. The inner electrode consists of a 150 mm long, 13 mm diameter stainless steel rod situated within a quartz tube, functioning as a high voltage inner electrode. A layer of stainless steel mesh is wrapped and secured around the quartz tube to serve as a low-pressure outside electrode. The experimental apparatus, illustrated in Fig. 1, comprises three primary components: flow rate regulation, DBD reactor, and gas detection. The feed gas CO_2 was provided by gas cylinders (purity: 99.99%, Shaanxi Lizhe Gas Technology Co., Ltd., China) and was introduced into the reactor following regulation of the flow rate using a pressure regulator valve and a mass flow controller (ACU10FD-LC, Beijing Precision Technology Co., Ltd., China). The product was subsequently collected at the outlet, and the flow rate was measured utilizing a soap film flow meter (GL-102B, Beijing Tianchuang Shangbang Instrument Co., Ltd., China). Finally, the gas-phase products were analyzed offline using a gas chromatograph (GC9790II, Zhejiang Fuli Analytical Instruments Co., Ltd., China) equipped with a thermal conductivity detector (TCD).

The CO_2 conversion rate is defined as follows:

$$CO_2\ conversion(\%)=\frac{n(CO_2)_{in}-n(CO_2)_{out}}{n(CO_2)_{in}}\times 100 \tag{1}$$

The CO yield is defined as follows:

$$CO\ yield(\%)=\frac{n(CO)}{n(CO_2)_{in}}\times 100 \tag{2}$$

The specific input energy (SIE) is defined as follows:

$$Specific\ input\ energy(\frac{kJ}{L})=\frac{P(W)}{F(CO_2)_{in}}\times 60 \tag{3}$$

Where P(W) represents the input power, $F(CO_2)_{in}$ (ml/min) denotes the inlet flow rate.

The energy efficiency (η) is defined as follows:

$$\eta(\%)=\frac{CO_2\ conversion\times\Delta H}{SIE\times 22.4} \tag{4}$$

where ΔH is the enthalpy of reaction for the decomposition of 1 mol CO2, ΔH = 283 kJ/mol.

The residence time (τ) is defined as follows:

$$\tau=\frac{\pi\times(R^2-r^2)\times d}{F(CO_2)_{in}}\times 60 \tag{5}$$

Where, R (mm) is the inner radius of the quartz tube, r (mm) is the radius of the stainless steel rod, and d (mm) is the length of the DBD discharge interval.

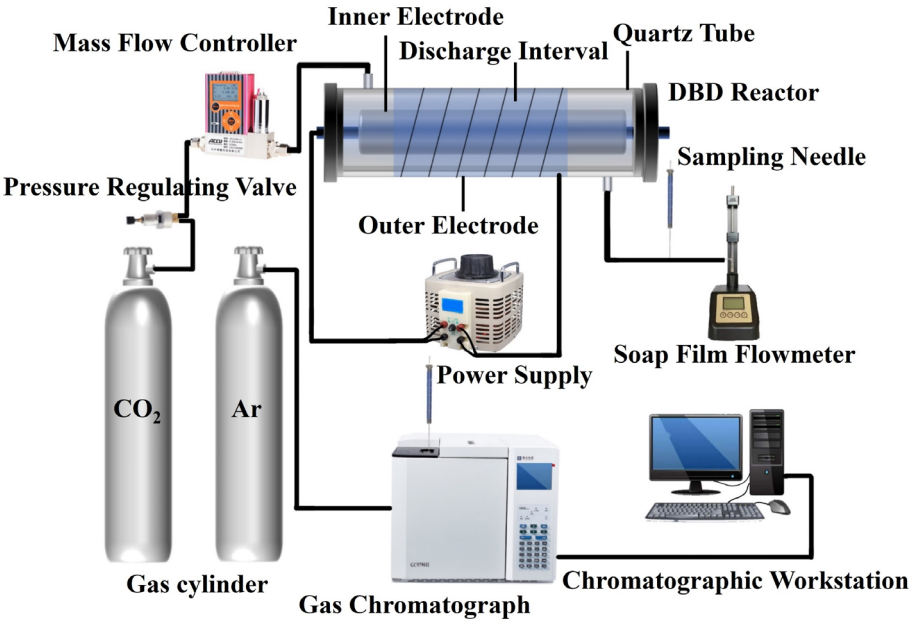

Fig. 1 Schematic diagram of the experimental device

2.3 Catalyst Characterization

X-ray diffraction (XRD) patterns of the samples were obtained utilizing a RIGAKU SMARTLAB diffractometer with a Cu Kα wavelength of 0.15418 nm, scanning at 2θ angles from 10° to 90°. The scanning velocity is 5 degrees per minute. Microscopic structural investigations were conducted using scanning electron microscopy (SEM, Hitachi SU8230). The surface chemistry of the foam metal was analyzed via X-ray photoelectron spectroscopy (XPS) utilizing a Thermofisher Nexsa model.

3. Results and Discussion

3.1 Effect of Iron Foam on CO_2 Conversion

The input power is a critical characteristic influencing plasma discharge. The studies included placing foam iron into the DBD discharge region and evaluating the influence of the filler material on CO_2 conversion efficiency at input powers of 35 W, 50 W, 65 W and 80 W. The experimental results are illustrated in Fig. 2.

The influence of input power on CO_2 conversion is illustrated in Fig. 2a. The experimental findings indicate that in the absence of any material in the reactor, CO_2 conversion rises with increasing input power, attaining 23% at an input power of 80 W. The primary reason for this is the rise in input power, resulting in heightened electron density in the discharge region, which produces more energetic electrons and enhanced the collisions between the carbon dioxide molecules and the energetic electrons, thereby increasing the rate of CO_2 conversion[12, 16]. The CO_2 conversion in IF-DBD was consistently greater, reaching up to 30%, under all fixed experimental circumstances compared to the

empty reactor, and exhibited a similar trend to that of the empty reactor. The incorporation of iron foam has resulted in a transformation of the plasma discharge pattern from the initial filamentary discharge to the current amalgamation of filamentary and surface discharges[4]. As the input power increases, it results in a heightened electron density and an augmented number of microdischarges, hence enhancing CO_2 conversion[7, 17]. Furthermore, the extensive porosity of the iron foam offers active sites and micro-reaction channels for CO_2 molecules, facilitating a sequence of processes including adsorption, conversion, and desorption on these sites and channels[5, 18], thereby enhancing CO_2 conversion.

Fig. 2b illustrates the impact on energy efficiency across the identical input power range. The figure illustrates that when the input power rises from 35 W to 80 W, the energy efficiency in the empty reactor grows from 1.06% to 1.3% before declining to 1.2%. In contrast, the energy efficiency in the IF-DBD diminishes from 2.0% to 1.6%. Initially, the absolute amount of CO_2 conversion escalates with the augmentation of input power, resulting in a preliminary gain in energy efficiency within an empty reactor[19]. As the reaction progresses, a portion of the energy within the reactor is utilized for CO_2 conversion, while the remainder is released as heat, causing an elevation in the reactor's internal temperature and a subsequent reduction in energy efficiency[20, 21].

Fig. 2c illustrates the impact of input power on CO yield. The CO yield rose with the rise in input power, and the CO yield were greater in the IF-DBD compared to the empty reactor. At 80 W, the CO yield in the IF-DBD reached 26%, while it was 22% in the empty reactor. It can also be observed from Fig. 2c illustrates that the CO yield growth rate progressively diminishes in IF-DBD. Due to the rise of input power, the absolute conversion of CO_2 increases, but at the same time, the reverse reaction rate between CO and O_2 also increases, leading in a drop in the growth rate of CO yield[13, 22, 23].

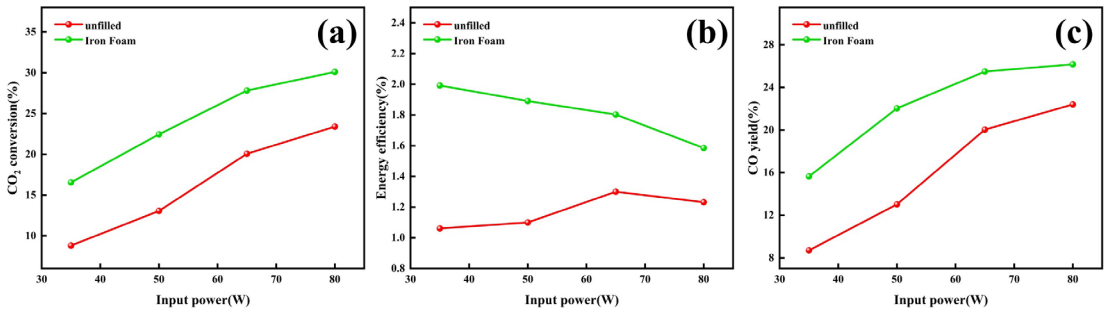

Fig. 2 Effect of input power on CO_2 conversion performance (a) CO_2 conversion; (b) energy efficiency; (c) CO yield

3.2 Thermal Stability Test

Temperature, an important factor influencing reaction rates, can result in catalyst fragmentation and deactivation upon reaching a specific threshold. To evaluate the thermal stability of the iron foam, it was positioned in a DBD reactor, and experiments were conducted continuously at a constant output of 80 W. The CO_2 variations were tested at 30-minute intervals, and the experimental results are presented in Fig. 3.

Fig. 3a illustrates that the utilization of foamed iron initially increases CO_2 conversion, subsequently stabilizes temporarily, and then gradually declines until reaching a plateau. Three phases of iron foam are evident: the activation phase, the stabilization phase, and the decay phase. From 0 h to 2.5 h, the iron foam had an activation phase, during which the CO_2 conversion rate progressively rose as the reaction advanced. At 2.5 h, the iron foam began to attain the stable phase, which continued until 3.5 h. The steady phase lasted a shorter duration, during which the CO_2 conversion rate reached 28.4%. From 3.5 h onwards, the iron foam enters the decline phase, during which the CO_2 conversion rate progressively diminishes as the reaction advances. At 5.5 h, the CO_2 conversion stabilized at 20%. The CO_2 conversion exceeded that of the empty reactor during both the activation and stabilization phases of the iron foam catalysts; however, the CO_2 conversion of the IF-DBD initially surpassed that of the empty reactor during the decay phase, subsequently declining until it fell below that of the empty reactor.

Fig. 3b illustrates the correlation between energy efficiency and reaction time. In IF-DBD, energy efficiency has a similar trend to the CO_2 conversion rate, reaching up to 1.5%. Conversely, in the empty reactor, the energy efficiency attains merely 1.2%. The temperature in the discharge zone of the DBD reactor increases more rapidly with continuous application of 80 W of power, resulting in greater energy dissipation as heat, hence reducing energy efficiency.

Fig. 3c illustrates the correlation between CO yield and reaction time. In the IF-DBD, the CO yield initially rose and thereafter declined with the reaction time. After 3.5 hours, the CO yield was progressively inferior to that of the vacant reactor. The primary reason is that elevated input power can raise the temperature, which adversely impacts the discharge efficiency and discharge uniformity of the DBD reactor[8, 12], leading to a reduction in CO_2 conversion and thus diminishing CO output.

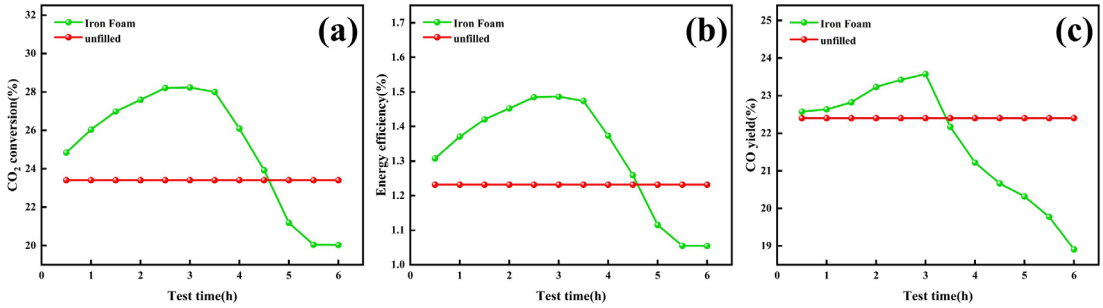

Fig. 3 Effect of the thermal stability of iron foam on CO_2 conversion performance: (a) CO_2 conversion; (b) Energy efficiency; (c) CO yield

3.3 Effect of Residence Time

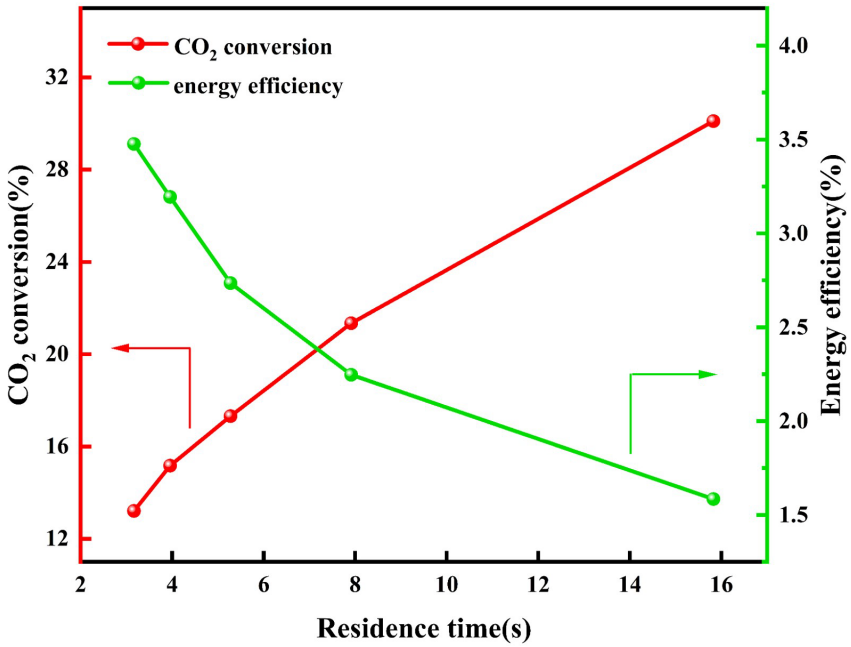

Fig. 4 Effect of residence time on CO_2 conversion efficacy of iron foam collaboration with DBD

Fig. 4 illustrates the effect of residence time on CO_2 conversion and energy efficiency in the IF-DBD reactor. The holding power is 80 W, and the residence time decreases with an increase in gas flow rate. As the inlet flow rate escalates from 20 ml/min to 100 ml/min, the residence time diminishes from 15.8 s to 3.1 s. The graphic illustrates that as residence time increases, the CO_2 conversion rate progressively rises. The extended residence time of CO_2 molecules in the discharge region of the DBD reactor enhances both the interaction probability between high-energy electrons and CO_2 molecules and the contact duration between CO_2 and iron foam, facilitating full decomposition and thereby increasing CO_2 conversion[24]. At the same time, the plasma voltage will vary as a result of alterations in flow velocity. A reduced flow rate results in elevated plasma voltage, generating a more intense electric field that accelerates high-energy electrons, thus enhancing the CO_2 conversion rate

at a diminished flow rate[12]. However, Increasing residence time can enhance CO_2 conversion, but it frequently results in reduced energy efficiency. At a residence time of 3.1 s, energy efficiency can attain 3.5%. Conversely, at a residence time of 15.8 s, energy efficiency declines to 1.5%. The energy efficiency is greater at elevated flow rates due to more complete utilization of the electrical energy provided to the reactor during a reduced residence time[22]. Furthermore, this can also be elucidated by Eq. (3) and Eq. (4). Eq. (3) indicates that SIE diminishes as the inlet flow rate escalates. According Eq. (4), a drop in SIE results in an increase in energy efficiency.

3.4 Characterization Analysis

Fig. 5a illustrates the XRD spectra of iron foam prior to and after to the reaction. The XRD pattern of Fe prior to the reaction exhibits two characteristic peaks with 2θ values of 45.3° and 65.7°, with the strongest characteristic peak corresponding to the Fe(110) crystal plane. In comparison to the pre-reaction state, post-reaction, a prominent characteristic peak emerged at 2θ = 45.2°, accompanied by a marked reduction in the intensity of its characteristic peak. Obviously, the main phase composition of iron foam is Fe.

Fig. 5b illustrates the XPS spectrum of Fe 2p. The principal peaks of Fe 2p, both prior to and subsequent to the reaction, are observed at binding energies of 724 eV and 711 eV, corresponding to Fe 2p1/2 and Fe 2p3/2[25, 26]. The peak of Fe^0 was observed at the binding energy of 718.2 eV and 731 eV[27], indicative of the metallic properties of Fe, and the binding energy position did not shift before and after the reaction. Furthermore, peaks of Fe^{2+} and Fe^{3+} are detectable on the surface of foamed iron both prior to and after to the reaction, primarily originating from iron oxides. Surface iron is more susceptible to environmental factors, and its exposure to air may result in little iron oxidation[28]. Following the DBD reaction, the iron surface is exposed to a high-temperature mixture of gases containing O_2, which may also cause surface oxidation. Obviously, due to the exceedingly low concentration of surface oxides in iron, it has not been detected in XRD[29].

Figs. 5c and 5d illustrate the SEM spectra prior to and subsequent to the reaction of iron foam, respectively. Iron foam is a material characterized by a three-dimensional network structure, exhibiting an irregular structure similar to honeycomb on the whole. As can be seen from Fig. 5c, the surface of the iron foam is coarse. In comparison to the pre-reaction, the SEM image of the iron foam after the DBD reaction exhibited significant alterations, as illustrated in Fig. 5d. Following the DBD reaction, the surface of the foamed iron exhibits pronounced cracks, accompanied by a flocculent structure at the fissures. This suggests that following DBD treatment, the surface morphology of foamed iron alters, leading to diminished stability[30].

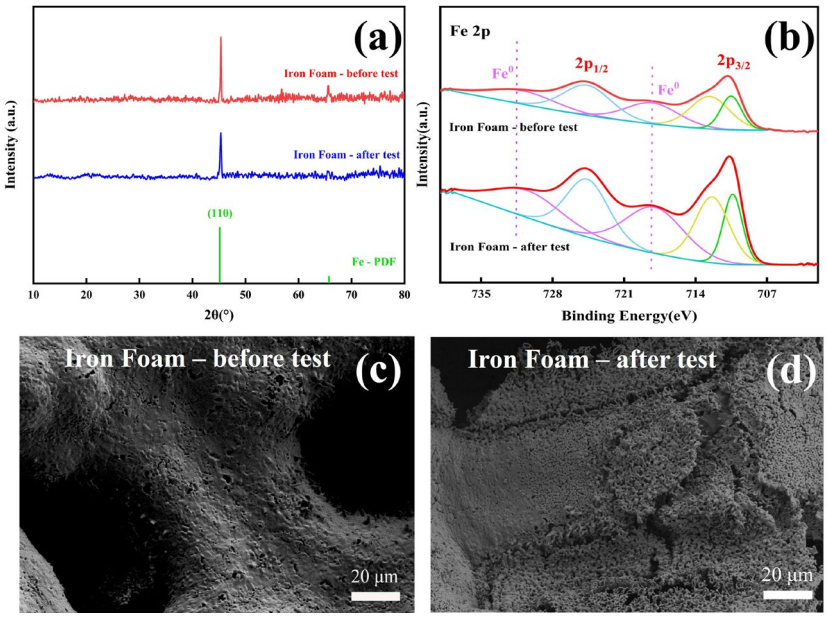

Fig. 5 (a) XRD spectra of iron foam; (b) Fe 2p XPS spectra of iron foam; (c) SEM image of iron foam before the reaction; (d) SEM image of iron foam after the reaction.

4. Investigation of reaction mechanism

4.1 Gas phase reaction

In the empty DBD reaction system, the reaction involving plasma within the reactor is a gas-phase reaction. The decomposition of CO_2 molecules under the influence of high-energy electrons primarily results from electron impact dissociation[31-33]. As shown in Eq. (6), the CO_2 molecule can be decomposed into CO and O. Consequently, an increase in power supplied to the reaction system elevates electron energy and electron density, thereby facilitating the transformation of CO_2 molecules into a bigger quantity of CO and O[14]. Given that CO molecules exhibit significant stability with a bond energy of 11.19 eV, and the average energy of DBD plasma ranges from 1 to 10 eV, further decomposition of CO molecules is challenging[34, 35]. But during a long residence time, a tiny quantity of CO molecules can still mix with O atoms to generate CO_2, thereby hindering the conversion of CO_2[14]. Nonetheless, the recombination process of the O atom is more probable than its interaction with the CO molecule[36]. Simultaneously, the O atom can react with CO_2 to enhance CO_2 conversion, hence increasing conversion efficiency[37].

$$e+CO_2 \rightarrow CO+O+e \tag{6}$$

4.2 Catalytic reaction

Upon filling the DBD reactor with iron foam, the system undergoes simultaneous gas phase reactions and gas-solid heterogeneous phase reactions. The integration of iron foam and DBD plasma can markedly enhance CO_2 conversion efficiency, primarily relying on three key mechanisms. The first is that the introduction of a catalyst can alter the discharge mode of DBD plasma. For example, Lu et al.[20] introduced K-doped g-C_3N_4/Al_2O_3 catalyst into the DBD reactor, resulting in a transition from filament-like discharge to filament-surface discharge. Li et al.[4] introduced metal foams into the discharge gap and discovered that in the reactor containing metal foams, the discharge mode is a hybrid of filament discharge and surface discharge of current. The second is that the iron foam exhibits excellent electrical conductivity, facilitating the generation of robust electric fields and an increased presence of high-energy electrons in its vicinity, hence enhancing electron impact collisions and improving the CO_2 conversion rate. The third mechanism is the foam metal's porous structure and elevated specific surface area, which offer reaction sites and reaction channels for the conversion of CO_2 molecules.

5. Conclusion

This study employed DBD plasma technique for filling the reactor with the iron foam catalyst to explored its effect on CO_2 conversion performance. In the empty reactor, the CO_2 conversion rate escalates with the augmentation of input power, attaining 23% at 80 W. Upon filling the iron foam, the CO_2 conversion rate reached at 30% at a power of 80 W. Despite achieving the greatest CO_2 conversion rate at 80 W of input power, the energy efficiency remains suboptimal. Conversely, at 35 W power, the energy efficiency of filled iron foam reaches 2.0%, surpassing that of the empty reactor. In addition, the thermal stability of iron foam was also explored. The results showed that the CO_2 conversion rate grew with the extension of reaction time, reached stability, and then steadily fell, and finally was lower than that of the empty reactor. In IF-DBD, the CO_2 conversion rate increases with the increase of residence time. The surface composition and shape of iron foam were analysed using XRD, XPS and SEM. Due to the porous three-dimensional structure of iron foam offers a reaction site for CO_2 conversion, resulting in showed excellent catalytic activity and improved CO_2 conversion performance.

Acknowledgments

This work was financially supported by the Natural Science Foundation of China (NSFC, No. 22109126), Shaanxi Province key research and development plan item (2024CY2-GJHX-72), Yulin

City science and technology plan project (2023-CXY-189), and Key Laboratory of Coal Resources Exploration and Comprehensive Utilization, Ministry of Land Resources (SMDZ-KF2024-3), Shaanxi Province Key Point Research and Development Project (2022GY-378)

References

[1] CASTRO-PARDO S, BHATTACHARYYA S, YADAV R M, et al. A comprehensive overview of carbon dioxide capture: From materials, methods to industrial status [J]. Materials Today, 2022.

[2] WANG Y, CHEN E, TANG J. Insight on Reaction Pathways of Photocatalytic CO_2 Conversion [J]. ACS Catalysis, 2022.

[3] WANG B, WANG X, ZHANG B. Dielectric barrier micro-plasma reactor with segmented outer electrode for decomposition of pure CO_2 [J]. Frontiers of Chemical Science and Engineering, 2020.

[4] LI J, ZHAI X, MA C, et al. DBD Plasma Combined with Different Foam Metal Electrodes for CO2 Decomposition: Experimental Results and DFT Validations [J]. Nanomaterials, 2019.

[5] ASHFORD B, WANG Y, POH C-K, et al. Plasma-catalytic conversion of CO_2 to CO over binary metal oxide catalysts at low temperatures [J]. Applied Catalysis B: Environment and Energy, 2020.

[6] RAY D, SAHA R, CH. S. DBD Plasma Assisted CO_2 Decomposition: Influence of Diluent Gases [J]. Catalysts, 2017, 7(9): 244.

[7] SHENGJIE Z H U, AMIN Z, FENG Y U, et al. Enhanced CO_2 decomposition via metallic foamed electrode packed in self-cooling DBD plasma device [J]. Plasma Science and Technology, 2019.

[8] ZHOU A, CHEN D, DAI B, et al. Direct decomposition of CO_2 using self-cooling dielectric barrier discharge plasma [J]. Greenhouse Gases: Science and Technology, 2017.

[9] MA X, LI S, RONDA-LLORET M, et al. Plasma Assisted Catalytic Conversion of CO_2 and H2O Over Ni/Al2O3 in a DBD Reactor [J]. Plasma Chemistry and Plasma Processing, 2018.

[10] DEY G R, KAMBLE S. Effects of electrode material and frequency on carbon monoxide formation in carbon dioxide dielectric barrier discharge [J]. Journal of CO_2 Utilization, 2020.

[11] OZKAN A, DUFOUR T, BOGAERTS A, et al. How do the barrier thickness and dielectric material influence the filamentary mode and CO2conversion in a flowing DBD? [J]. Plasma Sources Science and Technology, 2016.

[12] OZKAN A, BOGAERTS A, RENIERS F. Routes to increase the conversion and the energy efficiency in the splitting of CO_2 by a dielectric barrier discharge [J]. Journal of Physics D: Applied Physics, 2017.

[13] ZHANG K, HARVEY A P. CO_2 decomposition to CO in the presence of up to 50% O2 using a non-thermal plasma at atmospheric temperature and pressure [J]. Chemical Engineering Journal, 2020.

[14] RAY D, CHAWDHURY P, BHARGAVI K V S S, et al. Ni and Cu oxide supported γ-Al_2O_3 packed DBD plasma reactor for CO_2 activation [J]. Journal of CO_2 Utilization, 2020.

[15] MEI D, ZHU X, WU C, et al. Plasma-photocatalytic conversion of CO_2 at low temperatures: Understanding the synergistic effect of plasma-catalysis [J]. Applied Catalysis B: Environment and Energy, 2015.

[16] JAHANBAKHSH M R, TAGHVAEI H, KHALIFEH O, et al. Low-Temperature CO_2 Splitting in a Noncatalytic Dielectric-Barrier Discharge Plasma: Effect of Operational Parameters with a New Strategy of Experimentation [J]. Energy & Fuels, 2020.

[17] MEI D, TU X. Conversion of CO_2 in a cylindrical dielectric barrier discharge reactor: Effects of plasma processing parameters and reactor design [J]. Journal of CO_2 Utilization, 2017.

[18] VAN ‘T VEER K, ENGELMANN Y, RENIERS F, et al. Plasma-Catalytic Ammonia Synthesis in a DBD Plasma: Role of Microdischarges and Their Afterglows [J]. The Journal of Physical Chemistry C, 2020.

[19] NIU G, QIN Y, LI W, et al. Investigation of CO2 Splitting Process Under Atmospheric Pressure Using Multi-electrode Cylindrical DBD Plasma Reactor [J]. Plasma Chemistry and Plasma Processing, 2019.

[20] LU N, LIU N, ZHANG C, et al. CO_2 conversion promoted by potassium intercalated g-C3N4 catalyst in DBD plasma system [J]. Chemical Engineering Journal, 2021.

[21] NIU G, LI Y, TANG J, et al. Optical and electrical analysis of multi-electrode cylindrical dielectric barrier discharge (DBD) plasma reactor [J]. Vacuum, 2018.

[22] LU, NA, SUN, et al. CO2 conversion in non-thermal plasma and plasma/g-C3N4 catalyst hybrid processes [J]. Journal of Physics D Applied Physics A Europhysics Journal, 2018.

[23] YIN Y, YANG T, LI Z, et al. CO_2 conversion by plasma: how to get efficient CO_2 conversion and high energy efficiency [J]. Physical Chemistry Chemical Physics, 2021.

[24] DUAN X, LI Y, GE W, et al. Degradation of CO_2 through dielectric barrier discharge microplasma [J]. Greenhouse Gases: Science and Technology, 2014.

[25] KUMAR A, SHRIPATHI T, SRIVASTAVA P C. New insights into CoFe/n-Si interfacial structure as probed by X-ray photoelectron spectroscopy [J]. Journal of Science: Advanced Materials and Devices, 2016.

[26] FLAK D, CHEN Q, MUN B S, et al. In situ ambient pressure XPS observation of surface chemistry and electronic structure of α-Fe_2O_3 and γ-Fe_2O_3 nanoparticles [J]. Applied Surface Science, 2018.

[27] XIANG S, CHENG W, NIE X, et al. Zero-valent iron-aluminum for the fast and effective U(VI) removal [J]. Journal of the Taiwan Institute of Chemical Engineers, 2018.

[28] LIU Y, GONG X, HE R, et al. Stable Three-Dimensional Macroporous Iron-Foam Catalyst for Direct Conversion of CO2 to Olefins [J]. ACS Catalysis, 2024.

[29] ZHOU T, LIU Z, YANG B, et al. Dealloying fabrication of hierarchical porous Nickel–Iron foams for efficient oxygen evolution reaction [J]. Frontiers in Chemistry, 2022.

[30] HUANG Y, JIANG J, MA L, et al. Iron foam combined ozonation for enhanced treatment of pharmaceutical wastewater [J]. Environmental Research, 2020.

[31] KING S J, PRICE S D. Electron ionization of CO_2 [J]. International Journal of Mass Spectrometry, 2008.

[32] KEDZIERSKI W, BLEJDEA E, DICARLO A, et al. Electron impact dissociation of N_2O and CO2 with single particle detection of O(1D2) [J]. Chemical Physics Letters, 2010, 498(s 1–3): 38-41.

[33] MOSS M S, YANALLAH K, ALLEN R W K, et al. An investigation of CO_2 splitting using nanosecond pulsed corona discharge: effect of argon addition on CO_2 conversion and energy efficiency [J]. Plasma Sources Science and Technology, 2017.

[34] YAO Y, SHUSHKOV P, MILLER T F, et al. Direct dioxygen evolution in collisions of carbon dioxide with surfaces [J]. Nature Communications, 2019.

[35] ZHENG G, JIANG J, WU Y, et al. The Mutual Conversion of CO_2 and CO in Dielectric Barrier Discharge (DBD) [J]. Plasma Chemistry and Plasma Processing, 2003.

[36] YU Q, KONG M, LIU T, et al. Characteristics of the Decomposition of CO_2 in a Dielectric Packed-Bed Plasma Reactor [J]. Plasma Chemistry and Plasma Processing, 2011.

[37] RAY D, CHAWDHURY P, SUBRAHMANYAM C. A facile method to decompose CO_2 using a g-C3N4-assisted DBD plasma reactor [J]. Environmental Research, 2020.